압축기 토출벨브의 유체-구조 연계해석 및 충돌해석

Flow Structure Interaction 3-D Reciprocating Compressor and Impact Analyses of Compressor Discharge Valve

레사 옥타비안티* ·김동현† ·박강균* ·정원현·안재우·문경호·고영필·김형식**
Ressa Octavianty, Dong-Hyun Kim, Kang-Gyun Park,
Won-Hyun Jung, Jae-Woo Ahn, Kyeong-Ho Moon, Young-Pil Ko, and Hyeong-Sik Kim

Key Words : Flow-Structure Interaction(유체-구조 상호작용), Compressor(압축기), Discharge Valve(토출벨브), Impact Analysis(충돌해석), CFD(전산유체), FEM(유한요소법)

ABSTRACT

In this paper, 3-D reciprocating compressor is taken into flow-structure interaction analysis. The full cycle process consisted of cylinder expansion and compression has been modeled without considering flow leakage through cylinder wall. Fully-coupled FSI analysis of this compressor model was iteratively solved and gives sufficient result with the experimental test. The study is emphasized to thoroughly investigate discharge valve motion, opening and closing, in order to determine discharge valve region which is prone to have high effective stress. The cylinder pressure is successfully validated before conducting impact analyses between discharge valve and other susceptible supported structure. Velocity profile has been obtained in FSI analysis is used as initial condition to carry out further impact analyses. Stress result of discharge valve and valve spring gives preliminary estimation of higher stress area due to its impact phenomena.

1. Introduction

The recent extensive application of computer-aided design (CAD) has enabled many engineers to conduct viable analysis in estimating the performance of many vehicles, machine, and various manufactured design. The design of hermetic compressor for small refrigerator has been highlighted in recent analysis to progressively increase its reliability, durability, and efficiency during its operation. Thence, compressor modeling and simulation give insight into compressor performance and efficiency in its operating condition(1~6).

A new method of computer simulation(1) has been introduced to evaluate the working characteristic of air compressor by considering the pressure pulsation of suction vale and discharge valve. Moreover, unsteady one-dimensional model of compressor simulation code has been developed(2) in order to evaluate the mass flow rate, the electric power input, the heat flow rate, and the temperature inside compressor unit. Compressor analysis domain considering internal pressure waves(3) could accurately predict not only pressure distribution and gas flow, but also impact velocity and valve losses. More efficient computation using Warner's (4) algorithm is applied to solve the coupled problem between gas dynamic equation, acoustic plenum model, and valve dynamic model of refrigeration reciprocating compressor.

In this paper, we emphasize our analysis in scrutinizing discharge valve mechanism. Experimental test revealed that certain part of discharge valve prone to be exerted with high stress distribution due to its mechanism process. The discharge valve and other support components contribute to the life period of valve.

Within the compression stage, discharge valve failure is a common problem that makes compressor failed to operate whether we compare to another compressor component. Under normal operating condition, discharge valve may be failed by wear, overstress, fatigue, corrosion, or any combination of these factors(5).

In order to attain long-life operating cycle and valve reliability of the discharge valve, investigation on its opened-closed mechanism is necessarily needed. Flow-Structure Interaction analysis is required to simulate discharge valve moving mechanism. Based on velocity result which is given by FSI analysis, impact analyses is conducted to predict high-stress region at discharge valve structure.

† 정회원, 국립경상대학교 기계항공공학부 및 항공기부품기술연구소
E-mail : dhk@gsnu.ac.kr
Tel : (055) 751-6125, Fax : (055) 755-2081

* 정회원, 국립경상대학교 기계항공공학부 대학원
** LG 전자㈜ DAC 연구소

2. Computational Background

ADINA version 8.3 is commercial finite element software which provide powerful algorithm for solving various type of flow-structure interaction problem. In FSI analyses, fluid force gives deformation to structural model and this deformation changes fluid domain. The ALE formulation (Arbitrary Lagrangian Eulerian) at FSI boundary condition was imposed at the adjacent between fluid mesh and structure mesh although those are not compatible each other. Displacement and stress at fluid nodal at FSI boundary is determined by interpolating displacement and stress of solid node in the vicinity of corresponding fluid node[7,8].

2.1 Finite Element Equation of Iterative Fully-Coupled System

There are two basic conditions for applying fluid-structure interfaces. The first condition is kinematic condition or displacement compatibility which is presented as follow:

$$\underline{d}_f = \underline{d}_s, s \in N_s, f \in N_f \tag{1}$$

The second condition that must to be achieved is dynamic condition or traction equilibrium:

$$n \bullet \underline{\tau}_f = n \bullet \underline{\tau}_s, s \in N_s, f \in N_f \tag{2}$$

where $\underline{d}_f$ and $\underline{d}_s$ are the fluid and solid displacement respectively, and $\underline{\tau}_f$ and $\underline{\tau}$s, respectively, are the fluid and solid stresses, the fluid variables are denoted by *f* and the solid variables are denoted by s. The underlining characters denote that they are only defined in fluid-structure interfaces only.

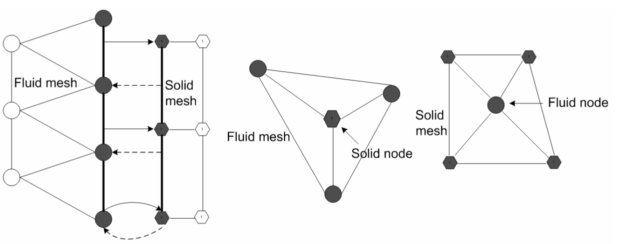

Fig. 1 Mapping fluid and solid nodes in FSI analysis

The mapping procedure between fluid and solid meshes is illustrated in Fig. 1 showed that incompatible meshes are applicable in FSI analysis. The algorithm for mapping operator could be stated in mathematics form as below:

$$\begin{aligned} M_{sf} &: \left\{ f_i \middle| i \in N_f \right\} \rightarrow \left\{ \hat{f}_i \middle| j \in N_s \right\} \\ M_{fs} &: \left\{ s_j \middle| j \in N_s \right\} \rightarrow \left\{ \hat{s}_j \middle| i \in N_f \right\} \end{aligned} \tag{3}$$

In order to resolve the response in flow-structure interaction analysis of compressor model, the governing equation of ALE formulation has been solved by iterative fully-coupled system. In this solution method, the latest information of one part coupled system is used to iterate another part of the system equation.

2.2 Nonlinear Dynamic Analysis

Implicit time integration method was imposed to solve impact analysis model. By applying the incremental finite element equilibrium equation, nonlinear dynamic analysis is carried out. Without equilibrium equation, implicit time integration could be stated as below:

$$M^{t+\Delta t}\ddot{U} + C^{t+\Delta t}\dot{U} + {}^{t}KU = {}^{t+\Delta t}R - {}^{t}F \tag{4}$$

If the equilibrium iteration is performed, the governing equation becomes:

$$M^{t+\Delta t}\ddot{U}^{(i)} + C^{t+\Delta t}\dot{U}^{(i)} + {}^{t+\Delta t}K\Delta U^{(i)} = {}^{t+\Delta t}R - {}^{t+\Delta t}F^{(i-1)} \tag{5}$$

where ${}^{t+\Delta t}\ddot{U}^{(i)}$, ${}^{t+\Delta t}\dot{U}^{(i)}$, ${}^{t+\Delta t}U^{(i-1)} + \Delta U^{(i)}$ are the approximations to the accelerations, velocities, and displacements obtained in iteration (*i*) respectively. And $M^{t+\Delta t}$, $C^{t+\Delta t}$, and ${}^{t+\Delta t}K$ are the mass matrix, the damping matrix, and the stiffness matrix at corresponding time $t + \Delta t$ respectively; ${}^{t+\Delta t}R$ and ${}^{t+\Delta t}F^{(i-1)}$ are the externally applied load vector at time $t + \Delta t$ and the consistent nodal force vector corresponding to the element stresses due to the displacement vector ${}^{t+\Delta t}U^{(i-1)}$ respectively.

In implicit time integration method, the convergence criteria used for all degree of freedom is energy convergence criterion which is described as:

$$\frac{\Delta U^{(i)^T} = \left[{}^{t+\Delta t}R - M^{t+\Delta t}\ddot{U}^{(i-1)} - C^{t+\Delta t}\dot{U}^{(i-1)} - {}^{t+\Delta t}F^{(i-1)} \right]}{\Delta U^{(1)^T} \left[{}^{t+\Delta t}R - M^{t+\Delta t}\ddot{U}^{(0)} - C^{t+\Delta t}\dot{U}^{(0)} - {}^{t}F \right]} \leq ETOL \tag{6}$$

Also, force and moment convergence criterion must be considered in nonlinear dynamic analysis. For the translational degrees of freedom, the notation is:

$$\frac{\left\| {}^{t+\Delta t}R - M^{t+\Delta t}\ddot{U}^{(i-1)} - C^{t+\Delta t}\dot{U}^{(i-1)} - {}^{t+\Delta t}F^{(i-1)} \right\|_2}{RNORM} \leq RTOL \tag{7}$$

For the rotational degrees of freedom, the notation is:

$$\frac{\left\| {}^{t+\Delta t}R - M\, {}^{t+\Delta t}\ddot{U}^{(i-1)} - C\, {}^{t+\Delta t}\dot{U}^{(i-1)} - {}^{t+\Delta t}F^{(i-1)} \right\|_2}{RMNORM} \le RTOL \tag{8}$$

3. Simulation Model of Reciprocating Compressor Analysis

We are interested in simulating valve motion during compressor reciprocated cycle through crankshaft mechanism, either expansion and compression stage. The reference is started from closed position of both suction valve and discharge valve. During the simulation, cylinder is obliged to carry out one full cycle expansion and compression.

3.1 Valve Dynamics

The valves motion, suction valve and discharge valve, are determined by the fluid pressure acting around it, upper part valve pressure and lower part valve pressure. The initial position of discharge valve is specified by preliminary gap distance exists to control the opening-closing valve mechanism. The gap has been resided to preclude numerical instability in fluid analysis domain. The valve dynamic equation could be stated as follow:

$$[M]\{\ddot{U}(t)\} + [C]\{\dot{U}(t)\} + [K]\{U(t)\} = A_f \Delta P(t) \tag{9}$$

where $[M]$ is the valve mass matrix, $[C]$ is the valve damping matrix, $[K]$ is the valve stiffness matrix, A_f is the effective flow area, $\Delta P(t)$ is the instantaneous pressure difference between upward and downward part of discharge valve, $\ddot{U}$ is the matrix acceleration, $\dot{U}$ is the matrix velocity, and U is the matrix position.

The reference of valve dynamics is of static equilibrium at closed position. Initial pre-load valve spring configuration has been determined by retainer suppression and its dynamic motion could be noted in matrix form as:

$$[M_{sp}]\{\ddot{U}(t)\} + [C_{sp}]\{\dot{U}(t)\} + [K_{sp}]\{U(t)\} = A_f \Delta P(t) + F_{pre} \tag{10}$$

where $[M_{sp}]$ is the spring mass matrix, $[C_{sp}]$ is the valve damping matrix, $[K_{sp}]$ is the valve stiffness matrix, A_f is the effective flow area, $\Delta P(t)$ is the instantaneous pressure difference between upward and downward part of discharge valve, and F_{pre} is the pre-load force.

The mass flow through the discharge valve could be presented in equation St.Venant and Wantzell below:

$$\dot{m}_d = \phi \rho_1^0 \left(\frac{P_2}{P_1^0}\right)^{\frac{1}{\gamma}} \sqrt{\frac{2\gamma}{\gamma-1}\frac{P_1^0}{\rho_1^0}\left(1-\left(\frac{P_2}{P_1^0}\right)^{\frac{\gamma-1}{\gamma}}\right)} \tag{11}$$

where $\dot{m}$ is the mass flow rate, P_2 is the averaged pressure in fore part of the valve, P_1 is the averaged pressure in aft part of the valve, γ is the ratio of specific heat, P_1^0 is the total pressure in aft part of discharge valve.

3.2 Complete System Considered

Fig.2 shows compressor part which is taken into analysis model. The model consists of several parts which are separately set up. The suction conduit conveys refrigerant from suction plenum to cylinder volume through suction valve is taken as initial point of gas flow. A discharge plenum including discharge valve is placed at the aft region of discharge valve. And also, a cylinder volume controls the expansion and compression pressure is set at the rear model part.

In this analysis compressor model is divided into 2 analysis domains, the fluid domain and the corresponding structural domain. The fluid domain relevantly includes all of region passed by refrigerant gas, such suction conduit, cylinder volume, discharge plenum, and discharge conduit. Particularly, the structural domain is comprised of suction valve, discharge valve, valve spring, retainer, and ring-mounted structure.

By assuming low-speed compressible flow to fluid domain, implicatively the flow exhibits Navier-Stokes equation:

$$\begin{aligned} &\frac{\partial \rho}{\partial t} + \nabla \bullet (\rho \vec{v}) = 0 \\ &\frac{\partial \rho \vec{v}}{\partial t} + \nabla \bullet (\rho \vec{v} v - \tau) = f^B \\ &\frac{\partial \rho E}{\partial t} + \nabla \bullet (\rho \vec{v} E - \tau \bullet v + q) = f^B \bullet \vec{v} + q^B \end{aligned} \tag{12}$$

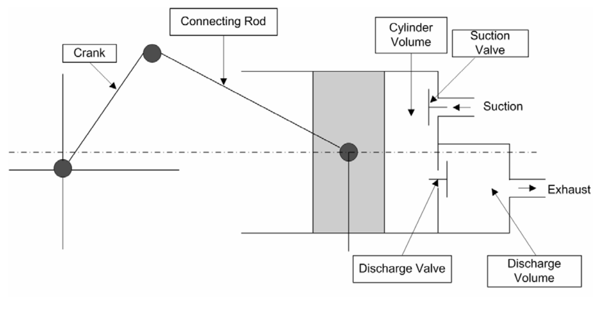

Fig.2 Schematic of compressor analysis model

where t is the time, ρ is the density, $\vec{v}$ is the velocity vector $\vec{v} = (u_x, u_y, u_z)$, f^B is the body force vector of fluid medium, τ is the fluid tensor, E is the specific total energy, and q is the heat flux, and q^B is the specific rate of heat generation.

The specific total energy and stress are defined as:

$$E = \frac{1}{2}\vec{v} \bullet \vec{v} + e \equiv b + e$$

$$\tau = (-p + \lambda \nabla \bullet v)\mathrm{I} + 2\mu u \tag{13}$$

where e is the specific internal energy, b is the specific kinetic energy, p is the pressure, μ and λ are the two coefficients of fluid viscosity, and u is the velocity strain tensor.

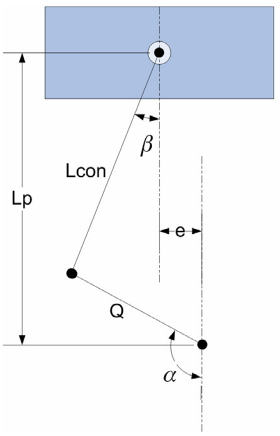

Fig.3 Piston moving mechanism

The heat flow is defined as follow:

$$q = -k\nabla\theta \tag{14}$$

where θ is the temperature and k is the heat conductivity coefficient.

In order to obtain the closed system of equation, the state equation is inquired to establish closed system which is defined as:

$$\rho = \rho(p,\theta) \qquad e = e(p,\theta) \tag{15}$$

The reciprocating compressor cylinder volume varies along time based on instantaneous piston position. Maximum cylinder compression has left a clearance volume of 0.4% to the cylinder stroke. No leakage is assumed between the cylinder chamber and its wall. The driving mechanism of compression stage is represented by the preceding Fig. 3 and denoted by the equation :

$$\begin{aligned} &L_p = L_{con}\cos\beta + Q\cos(180-\alpha), \\ &Q\sin\alpha - e = L_{con}\sin\beta \\ &\beta = \sin^{-1}\left[\frac{Q\sin(180-\alpha-e)}{L_{con}}\right] \end{aligned} \tag{16}$$

3.3 Finite Element of Discretization System

Fluid domain compressor model is divided into two primary parts, the cylinder part and the discharge plenum. Between those parts, gap boundary condition was imposed to segregate high pressure region in discharge volume and low pressure region inside cylinder. Slipping boundary condition is applied on outer surface of cylinder region to maintain good mesh quality as cylinder move forward, which is described as:

$$u_x = u, \qquad u_y = 0, \qquad u_z = 0 \tag{17}$$

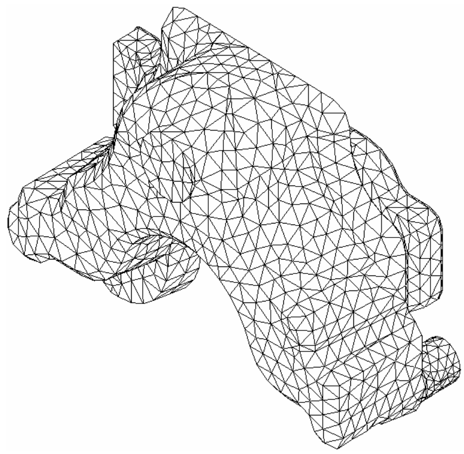

(a) Finite element model of compressor fluid domain (forefront view)

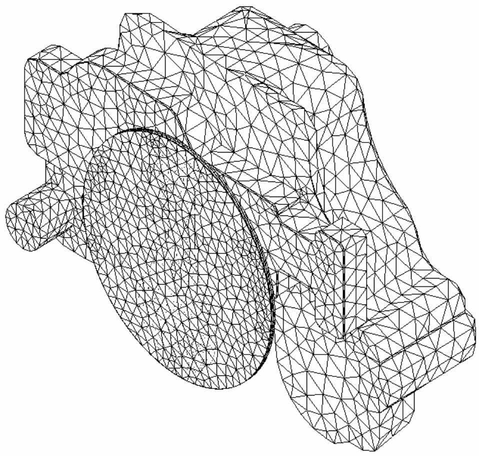

(b) Finite element model of compressor fluid domain (rearside view)

Fig.4 Automatic mesh generation of fluid domain

FSI boundary is imposed on corresponding area of fluid and structure. The fluid domain is discretized using 4-node tetrahedral 3-D fluid element by automatic mesh generation which is also shown in Fig.4a and 4b.

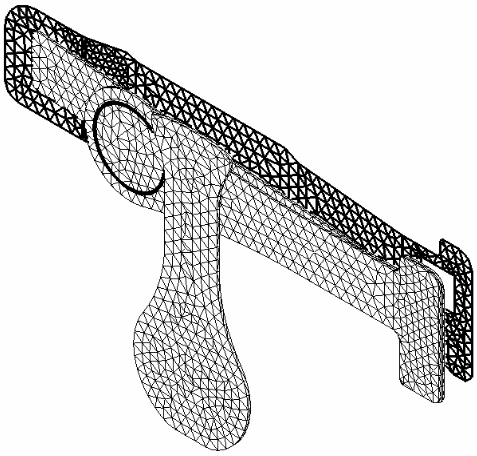

Fig.5 Automatic mesh generation of structural domain

The working fluid which is defined in this analysis is refrigerant gas. Material properties of fluid are presented in Table 1. In low speed compressible flow, the ideal gas law, $p = (C_p - C_v)\rho\theta$ and $e = C_v\theta$ is used to solve gas flow equation. The pressure ratio between compression and expansion inside cylinder is about 1:13. The compression speed of the present cylinder model is 3,636 rpm. The material properties data is calculated by using EES Program which is based on state equation [9].

The discharge valve mesh configuration is presented in Fig.5. In FSI analysis, structural model is discretized using 10-node tetrahedral 3-D solid element. Fixity was imposed at the root surface of valve as follow:

$$U_x = U_y = U_z = 0 \tag{18}$$

Material properties used in structural element are constant material as displayed in following Table 2.

Table 1 Material Properties of Refrigerant

Material Constant	R134a (P=115 kPa, T=331^{o}K)
Density (ρ)	4.335 kg/m^3
Viscosity (μ)	1.317e-5 kg/ms
Heat conductivity (k)	0.01641 W/mK
Coefficient of volume expansion (β)	0.003365 1/K
Specific heat at constant pressure (C_p)	919.1 m^2/s^{2}K
Specific heat at constant volume (C_v)	823.7 m^2/s^{2}K

Table 2 Material Properties of Structural Model

Suction valve	Discharge valve	Valve spring
E = 210 GPa	E =210 GPa	E = 210 GPa
v = 0.29	v = 0.29	v = 0.29
ρ = 7700 kg/m3	ρ = 7900 kg/m3	ρ = 7900 kg/m3

4. Result and Discussion

FSI analysis of compressor model has been conducted to simulate valve motion in its operating condition. The calculation is set off with cylinder expansion stage.

This analysis consumes about 50 hours of computational time. It consists of 30,803 elements and 7,002 nodes of 3-D fluid elements. The structural domain consists of 5,519 elements and 13,366 nodes. The simulation was performed using dual processors 3.2 GHz CPU, 2GB RAM with more than 2,500 time steps over one full expansion and compression cycle. In its expansion stage, suction valve is opened, which of through it, the refrigerant flow into cylinder volume. While its compression stage, the refrigerant flows out from cylinder volume into discharge plenum. The gap which separates those regions with different pressure control refrigerant flow in and out of cylinder.

4.1 Cylinder average pressure

Piston movement gives high increment to cylinder pressure. Fig.6 shows comparison graph of average pressure inside cylinder along expansion and compression cycle. While cylinder moved from its top position to bottom dead position (maximum compressed position), the gas exit through discharge valve as superheated vapor. The inclination slope reveals good agreement with experiment measurement. Averaged pressure in cylinder continuously increased until it reaches peak value at time = 0.0158 and begins to plunge. Simulation result gives discrepancies to the peak value. Prior to its cycle, the heat as of energy transfer taken place in system boundary of compressor toward outside system does not consider in this simulation. Heat transfer effect contributes in pressure loss of cylinder cycle. The further investigation on this must be carried out in order to optimize the compressor performance and work efficiency.

4.2 Valve lift due to compressor cycle

The suction valve lift displayed in Fig.7 shows 3 times opening stage during cylinder expansion. It must be noted that suction valve attachment is purposed to increase numerical stability in this simulation. Because we are only interested in investigating discharge valve motion and impact, the discussion about suction valve is left behind.

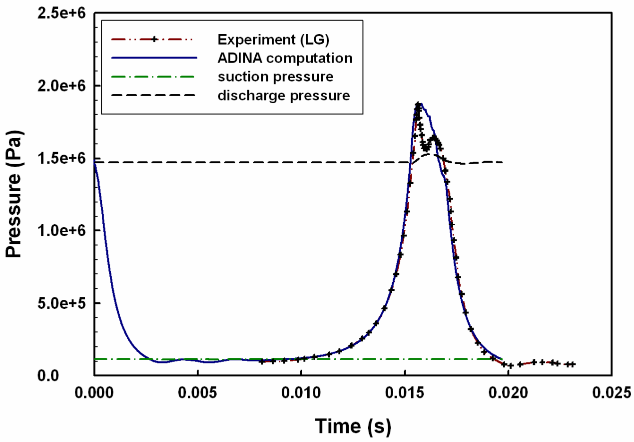

Fig.6 Average pressure of compressor cylinder

The discharge valve lift displacement which is shown in Fig.8 gives quantitative displacement result relative with time. The opened-closed time of discharge valve is controlled by a gap placed at aft discharge plenum.

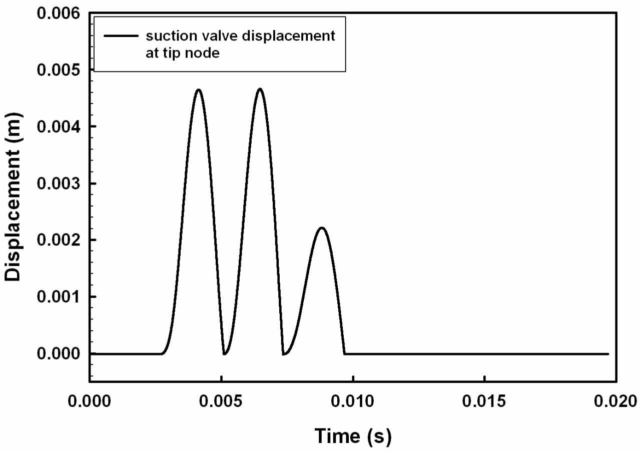

Fig.7 Suction valve lift due to pressure differences

Fig.8 reveals time range between fully opening valve position and fully closing valve position. Maximum valve lift gives maximum valve flow area which is occurred at time 0.01566. After reach the maximum displacement, the valve slightly moves backward due to the rebound force between valve spring and retainer. Energy releasing due to rebound force initiate forward motion of discharge valve. The closing position has been reached at time 0.01699 second.

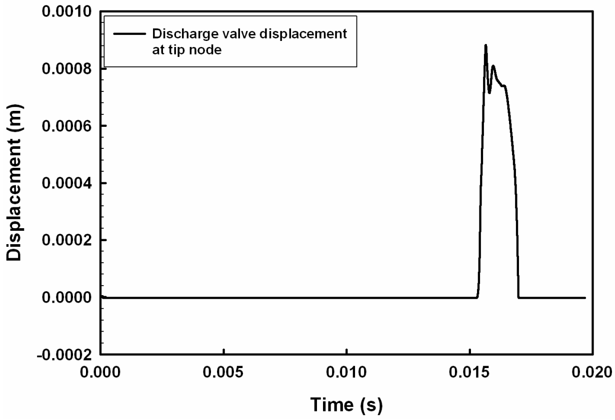

Fig.8 Discharge valve lift due to pressure difference

The refrigerant will surge into discharge plenum at valve opening stage. The valve non-ideality contributes to shutting-down process which it is not simultaneously closed when pressure difference occurs. Reverse crankshaft motion is set at time 0.0165, but the valve closing time occurs at time 0.01699. This non-ideality makes some amount of refrigerant flowing back from discharge plenum to cylinder volume.

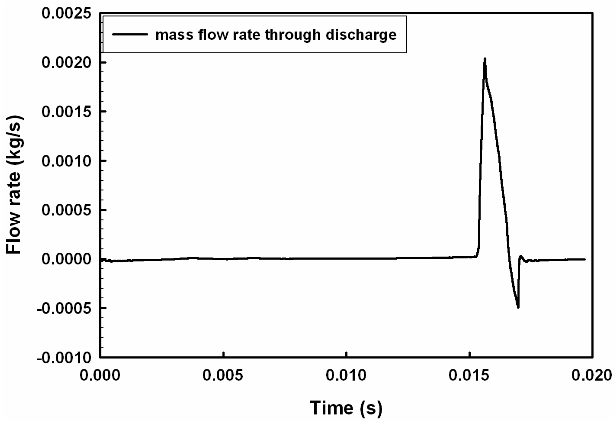

Fig.9 Flow rate through discharge conduit

Mass flow rate through discharge valve orifice could be depicted in Fig.9. Highest value of mass flow rate is about 0.002036 kg/s. The experiment measurement leads to the result of 0.00114 kg/s at discharge opening stage. Mean value of mass flow rate has been calculated based on the depicted graph. It notably gives the results of 0.001148 g/s. The negative value of mass flow rate is prior to shutting down delay of discharge valve.

4.3 Impact analyses

Based on FSI analysis result, velocity profile of discharge valve and other supported structure susceptible to impact is extracted to conduct further analysis. Those structures are restrained discharge valve to have unbounded motion. The impact will be considered to initially estimate failure probability around high stress region.

The following Fig.10 gives velocity contour of discharge valve just a moment before impact phenomenon. Maximum velocity remarks at the edge of discharge valve which results a value of 6.088 m/s. The effective stress value is obtained as impact result between discharge valve and pre-load valve spring.

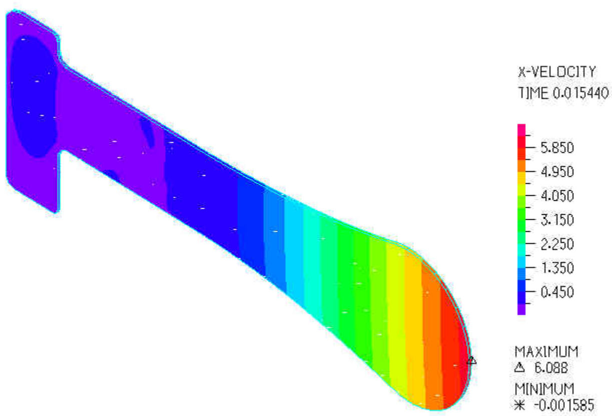

Fig.10 Discharge valve velocity contour before impact with discharge spring

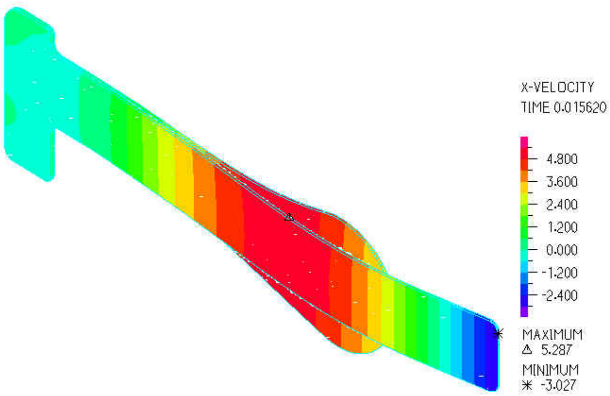

Fig.11 Valve spring velocity contour before impact with retainer

The preceding figure gives us a contour of valve spring velocity before impact with retainer. In spite of its pre-stress value at spring's throat, the middle region undergoes an impact velocity as could be seen in Fig.11. The highest velocity value before impact with retainer is about 5.287 m/s. Retainer structure sustains the end of valve spring in a fixed position and suppresses valve spring with pre-load stress.

For discharge valve closing mechanism, the velocity profile is presented in Fig.12. Maximum velocity is about 5.258 m/s at tip of discharge valve structure.

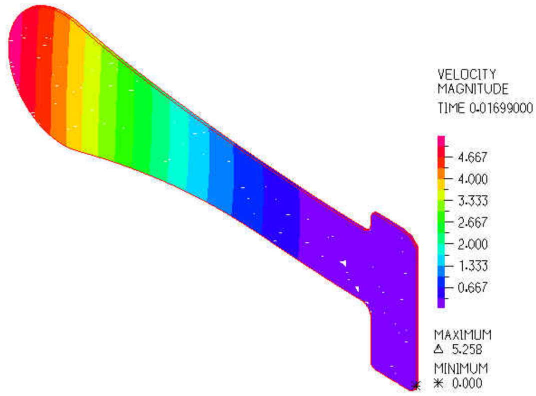

Fig.12 Discharge valve velocity contour before impact with ring-mounted structure

Impact analysis result for the first impact between discharge valve and valve spring shows tip impact on discharge valve. Impact stress contour is illustrated in Fig.13. The maximum effective stress is 213.7 MPa. This result is relatively low also it does not exceed the structural yield stress of discharge valve.

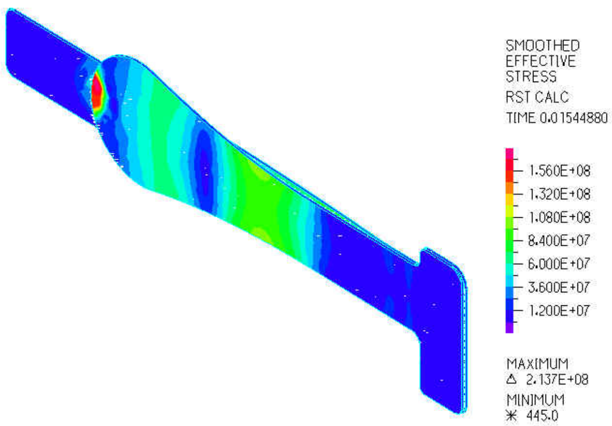

Fig.13 Effective stress due to impact between discharge valve and valve spring

Much higher stress result has been taken place at valve spring due to impact with retainer as described in Fig.14. It yields the value 840.6 MPa. This higher result compare to the first impact is related to rigid impact exerted between elastic structure of valve spring and rigid structure retainer. This value is still below the critical failure stress due to fatigue.

Fig.15 shows effective stress result due to impact with ring-mounted structure. Maximum stress value for this result is 234.7 MPa. This impact has been occurred with half region of ring-mounted structure due to slightly bend impact position of discharge valve.

Based on stress contour results obtained from impact analyses, we deduce that discharge valve and its supported structure configuration could achieve the long durability in its operating cycle.

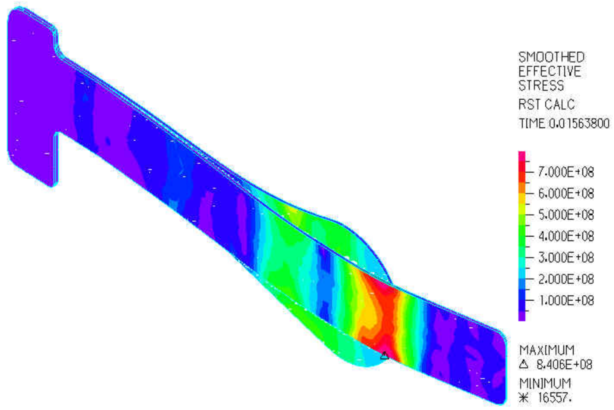

Fig.14 Effective stress due to impact between valve spring and retainer

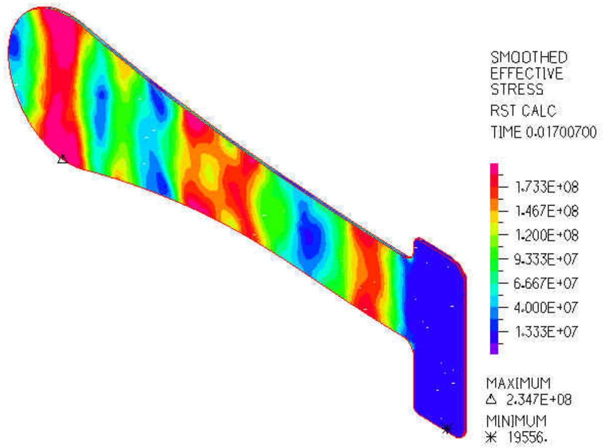

Fig.15 Effective stress due to impact between valve spring and retainer

5. Conclusion

Flow Structure Interaction Analysis gives a reliable comparison result with experimental test. The pressure losses during this simulation have been arisen because heat convection between cylinder volume and its wall does not take into analysis consideration. Nevertheless, its contribution to impact velocity does not give a massive effect. Impact analysis corresponded to FSI velocity result data could estimate critical region of high effective stress at either discharge valve and valve spring configuration. Objectively, heat transfer effect is needed to be considered in order to investigate compressor performance in several operating condition as well as the leakage in compressor performance.

Acknowledgement

This works was supported by LG Electronics Ltd., NURI and 2nd stage BK21 Projects.

References

[1] Sun, S.Y., Ren, T.R., 1995, “New Method of Thermodynamic Computation for a Reciprocating Compressor: Compressor Simulation of Working Process,” International Journal of Mechanical Sciences, Vol. 37, No. 4, pp. 343~353.

[2] Longo, G.A., Gasparella, A., 2003, “Unsteady State Analysis of the Compression Cycle of a Hermetic Reciprocating Compressor,” International Journal of Refrigeration, Vol. 26, pp. 681~689.

[3] Aigner, R., Meyer, G., Steinrück, H., 2005, “Valve Dynamics and Internal Waves in a Reciprocating Compressor,” 4th Conference of EFRC.

[4] Srinivas, M.N., Padmanabhan, C., 2002, “Computationally Efficient Model for Refrigeration Compressor Gas Dynamics,” International Journal of Refrigeration, Vol. 25, pp. 1083-1092.

[5] Woollatt, D., 2003, “Reciprocating Compressor Valve Design: Optimizing Valve Life and Reliability,” Technical Report.

[6] Flade, G., Will, G., Steinrück, H., 2004, “Initial Opening of a Compressor Valve,” Proceedings in Applied Mathematics and Mechanics, Vol. 4, pp. 434~435.

[7] ADINA R&D Inc., 2003, ver.8.3, Theory and Modeling Guide.

[8] Bathe, K.J., 1996, Finite Element Procedures, Prentice-Hall.

[9] F-Chart Software, 2006, Engineering Equation Solver Manual.